Electron Microscopic Visualization of Sites of Nascent DNA Synthesis by Streptavidin-Gold Binding to Biotinylated Nucleotides Incorporated In Vivo

K. T. Hiriyanna,* J. Varkey,‡ M. Beer,‡ and R. M. Benbow*

*Department of Zoology and Nucleic Acid Facility, Iowa State University of Science & Technology, Ames, Iowa 50011-3223; and ‡Department of Biophysics, The Johns Hopkins University, Baltimore, Maryland 21218

Abstract. Biotinylated nucleotides (bio-11-dCTP, bio-11-dUTP, and bio-7-dATP) were microinjected into unfertilized and fertilized *Xenopus laevis* eggs. The amounts introduced were comparable to in vivo deoxynucleoside triphosphate pools. At various times after microinjection, DNA was extracted from eggs or embryos and subjected to electrophoresis on agarose gels. Newly synthesized biotinylated DNA was analyzed by Southern transfer and visualized using either the BluGENE or Detek-hrp streptavidin-based nucleic acid detection systems. Quantitation of the amount of biotinylated DNA observed at various times showed that the microinjected biotinylated nucleotides were efficiently incorporated in vivo, both into replicating endogenous chromosomal DNA and into replicating microinjected exogenous plasmid DNA. At least one biotinylated nucleotide could be incorporated in vivo for every eight nucleotides of DNA synthesized. Control experiments also showed that heavily biotinylated DNA was not subject to detectable DNA repair during early embryogenesis (for at least 5 h after activation of the eggs). The incorporated biotinylated nucleotides were visualized by electron microscopy by using streptavidin-colloidal gold or streptavidin-ferritin conjugates to bind specifically to the biotin groups projecting from the newly replicated DNA. The incorporated biotinylated nucleotides were thus made visible as electron-dense spots on the underlying DNA molecules. Biotinylated nucleotides separated by 20–50 bases could be resolved. We conclude that nascent DNA synthesized in vivo in *Xenopus laevis* eggs can be visualized efficiently and specifically using the techniques described.

THE ability to easily localize, at high resolution, sites of nascent DNA synthesis on DNA molecules replicating in vivo would represent a major technical advance relevant to many areas of cell biology. Currently, single- and double-stranded DNA molecules can be readily distinguished from each other by electron microscopy (15). This technique does not, however, distinguish between nascent and preexisting DNA. Newly synthesized DNA can be visualized as a track of silver grains by light microscopy using DNA fiber autoradiography (24, 25; reviewed in references 16 and 23). The DNA strands that give rise to the grain tracks, however, cannot be resolved. Nascent DNA has been observed also by electron microscope DNA fiber autoradiography (38). This technique is technically demanding and has only limited resolution (better than 0.25 μM; i.e., 750 bp).

The high affinity of avidin (20) and streptavidin (14) for biotin provides a theoretical basis for visualizing nascent DNA in the electron microscope. Biotinylated analogs (29) of deoxyribonucleoside triphosphates, the normal precursors of DNA synthesis, and electron-dense streptavidin-colloidal gold and streptavidin-ferritin conjugates have recently become commercially available. Prokaryotic and eukaryotic DNA polymerases have been shown to incorporate biotinylated nucleoside triphosphates into DNA in vitro at 30–40% of the normal rate (29). Moreover, incorporated biotinylated nucleotides can be visualized on gels using commercially available streptavidin-based detection systems. These systems have been used successfully to detect specific DNA sequences with biotinylated DNA or RNA probes (30). Avidin- and streptavidin-gold conjugates also have been used for the high resolution electron microscopy of biotinylated probes hybridized in situ to specific sequences on metaphase chromosomes (21, 35).

To use biotinylated nucleotides to visualize nascent DNA synthesized in vivo, it is first necessary to show that the biotinylated derivatives do not significantly perturb normal DNA replication. Several criteria must be satisfied. (*a*) The biotinylated nucleotides must be incorporated in vivo efficiently with kinetics similar to the incorporation of unbiotinylated nucleotides; (*b*) the incorporated nucleotides must not be removed efficiently by DNA repair processes in vivo (i.e., the newly replicated DNA containing the biotinylated nucleotides must remain intact long enough to be visualized); and (*c*) the incorporated nucleotides must be detectable at

high resolution by electron microscopy. We demonstrate here that all of these conditions are met in microinjection experiments using *Xenopus laevis* embryos.

Materials and Methods

Reagents

Biotin-11-dUTP, biotin-7-dATP, φX174 DNA, Hind III restriction endonuclease, BluGENE[1] (Bethesda Research Laboratories, Gaithersburg, MD) nonradioactive nucleic acid detection system, and streptavidin-colloidal gold conjugate (20 nm) were obtained from Bethesda Research Laboratories (Gaithersburg, MD). Streptavidin-colloidal gold conjugates (5 and 10 nm) were from Sigma Chemical Co. (St. Louis, MO). Bio-11-dCTP and Detek-hrp kits were from Enzo Biochem Inc. (New York, NY). ^{32}P-labeled dATP and TTP (3,000 Ci/mmol) were from ICN Radiochemicals (Irvine, CA). pXGαβ1 (a gift from R. Patient), pX108, and pBR322 were purified in our laboratory by standard procedures (32). Oligonucleotide primers were synthesized on a DNA Synthesizer (model No. 8750; Biosearch, San Rafael, CA) and were purified by HPLC on a Vydac C4 column (l) by the Iowa State University Nucleic Acid Facility. *Escherichia coli* DNA polymerase I large fragment was from Promega Biotec (Madison, WI).

Microinjection of Nucleotides and DNA

Adult *Xenopus laevis* were acquired from Xenopus I (Ann Arbor, MI). Healthy female frogs were injected with human chorionic gonadotropin at least 12 h before they were stripped for eggs. The eggs were fertilized in 5% De Boers solution according to the procedure of Wolf and Hedrick (42). Both fertilized and unfertilized eggs were dejellied with 2% cysteine solution (pH 7.7) before they were microinjected according to the protocol of Gurdon (22). Unfertilized eggs were irradiated for 30 s with ultraviolet light (254 nm) to inactivate the female pronucleus before microinjection. Biotinylated and ^{32}P-radiolabeled nucleoside triphosphates were injected into the animal hemisphere with and without exogenous plasmid DNA in a total volume of 50 nl. The microinjected eggs and embryos were incubated for the specified times at 22°C in modified Barth's solution containing 5% Ficoll type 400 (Sigma Chemical Co.) (36).

Extraction of DNA and Visual Detection of Incorporated Nucleotides

DNA was extracted by gently crushing the eggs or embryos with a glass rod in an extraction buffer containing 50 mM EDTA, 20 mM Tris-HCl (pH 8.0), 1% SDS (Sigma Chemical Co.) followed by treatment with 500 μg/ml proteinase K for 3 h at 37°C. NaCl was added to a final concentration of 1.5 M, the sample was kept on ice for 1 h, then centrifuged. The DNA in the clear supernatant was precipitated with 2 vol of ethanol.

The precipitated DNA was dissolved in loading buffer and subjected to electrophoresis on 1% agarose gels. The DNA was transferred to nitrocellulose filters by blotting (32) and the incorporated biotinylated nucleotides were visualized using the BluGENE (Bethesda Research Laboratories) or Detek-hrp (Enzo Biochem, Inc., New York, NY) nonradioactive nucleic acid detection systems. For accurate quantitation, DNA was routinely titrated with respect to the extent of biotinylation and compared to known amounts of DNA synthesized in vitro containing known amounts of incorporated biotinylated nucleotides (see Fig. 4) in the gels or on the blots. To monitor the incorporation of ^{32}P-labeled nucleotides, autoradiograms were made using Kodak XAR5 x-ray film.

Preparation of Biotinylated φX174 DNA In Vitro

Biotinylated Form II φX174 DNA was prepared by synthesizing a complete complementary strand to φX174 viral (+) strand DNA which had been annealed to an oligonucleotide 25-mer primer complementary to a sequence close to the physiological replication origin. Primer extension was carried out at 18°C under conditions that enhanced full-length synthesis (41) in the presence of biotinylated nucleoside triphosphates (i.e., the synthesis was carried out with *E. coli* DNA polymerase large fragment in a reaction mixture where biotin-11-dUTP replaced thymidine triphosphate). The reactions were monitored by electrophoresis on agarose gels for the production of Form II φX174 DNA. Approximately 24% of the nucleotides on the complementary strand were expected to be biotinylated using this procedure.

End-labeling of restriction enzyme fragments with biotinylated nucleotides was carried out as described by Maniatis et al. (32) for end-filling with [^{32}P]dNTP.

Electron Microscopy and Detection of Incorporated Nucleotides Using Streptavidin-Colloidal Gold or Streptavidin-Ferritin Conjugates

DNA was further purified by HPLC on a Nucleogen DE-4000-IU column or by column chromatography on benzoylated naphthoylated DEAE cellulose (Boehringer Mannheim Biochemicals, Indianapolis, IN), or on low-temperature melting agarose gels. The purified DNA was suspended either in 10 mM Hepes (Sigma Chemical Co.) buffer (pH 7.5) containing 100 mM NaCl or in 100 mM Tris-HCl buffer (pH 7.5) containing 150 mM NaCl. Suitable concentrations of streptavidin-colloidal gold or streptavidin-ferritin conjugates were determined empirically for each sample of DNA. Samples were titrated with free biotin, when required, to reduce the number of ligand binding sites on the streptavidin-colloidal gold conjugates. The streptavidin-colloidal gold or streptavidin-ferritin conjugates and biotinylated DNAs were allowed to react for 15 min at room temperature and then spread for electron microscopy using the microdrop procedure of Lang and Mitani (28) or with the Kleinschmidt spreading procedures (27) using cytochrome c (15). Grids were stained with uranyl acetate, rotary shadowed with Pt-Pd (80:20), and photographed on Zeiss EM 109 or Philips 420 electron microscope, usually at a magnification of 7,000-20,000.

Results

Biotinylated Nucleotides Were Incorporated Efficiently into Plasmid and Endogenous High Molecular Weight DNA In Vivo

As shown in Fig. 1 *a*, biotinylated nucleotides were incorporated into both endogenous high molecular weight (chromosomal) DNA and plasmid DNA microinjected into unfertilized eggs and embryos. The rate of incorporation of biotinylated nucleotides closely paralleled the incorporation of coinjected ^{32}P-TTP in the same eggs and embryos (compare Fig. 1 *a* with the corresponding autoradiogram shown in Fig. 1 *b*). Embryos microinjected with up to 10 pmol each of bio-11-dCTP and bio-11-dUTP developed normally through at least the midblastula stage, although some exhibited abnormal morphology during late gastrulation. Incorporation into endogenous high molecular weight (chromosomal) DNA, which was present at far lower concentrations (6 pg/nucleus vs. 4 ng plasmid DNA/embryo), was nonetheless much more efficient than incorporation into microinjected plasmid DNA with either biotinylated or ^{32}P-labeled nucleoside triphosphates (see Discussion).

Microinjected single-stranded circular φX174 (+) strand DNA also served as an excellent template in unfertilized eggs for incorporation of biotinylated nucleoside triphosphates (Fig. 2). Within 1.5 h substantial incorporation of biotinylated nucleotides into molecules comigrating with fully double-stranded Form II DNA was observed. By 3 h after microinjection, DNA comigrating with Form I (supercoiled) φX174 DNA was the most heavily biotinylated species. These kinetics were not significantly different from those of single-stranded DNA replicated in unfertilized eggs into which biotinylated nucleoside triphosphates had not been injected (not shown).

These results establish that biotinylated nucleotides were incorporated in vivo into endogenous or plasmid DNA molecules without visibly interfering with early embryogenesis

1. BluGENE is a registered trademark of Bethesda Research Laboratories, Gaithersburg, MD. Detek-hrp is a registered trademark of Enzo Biochem Inc., New York, NY.

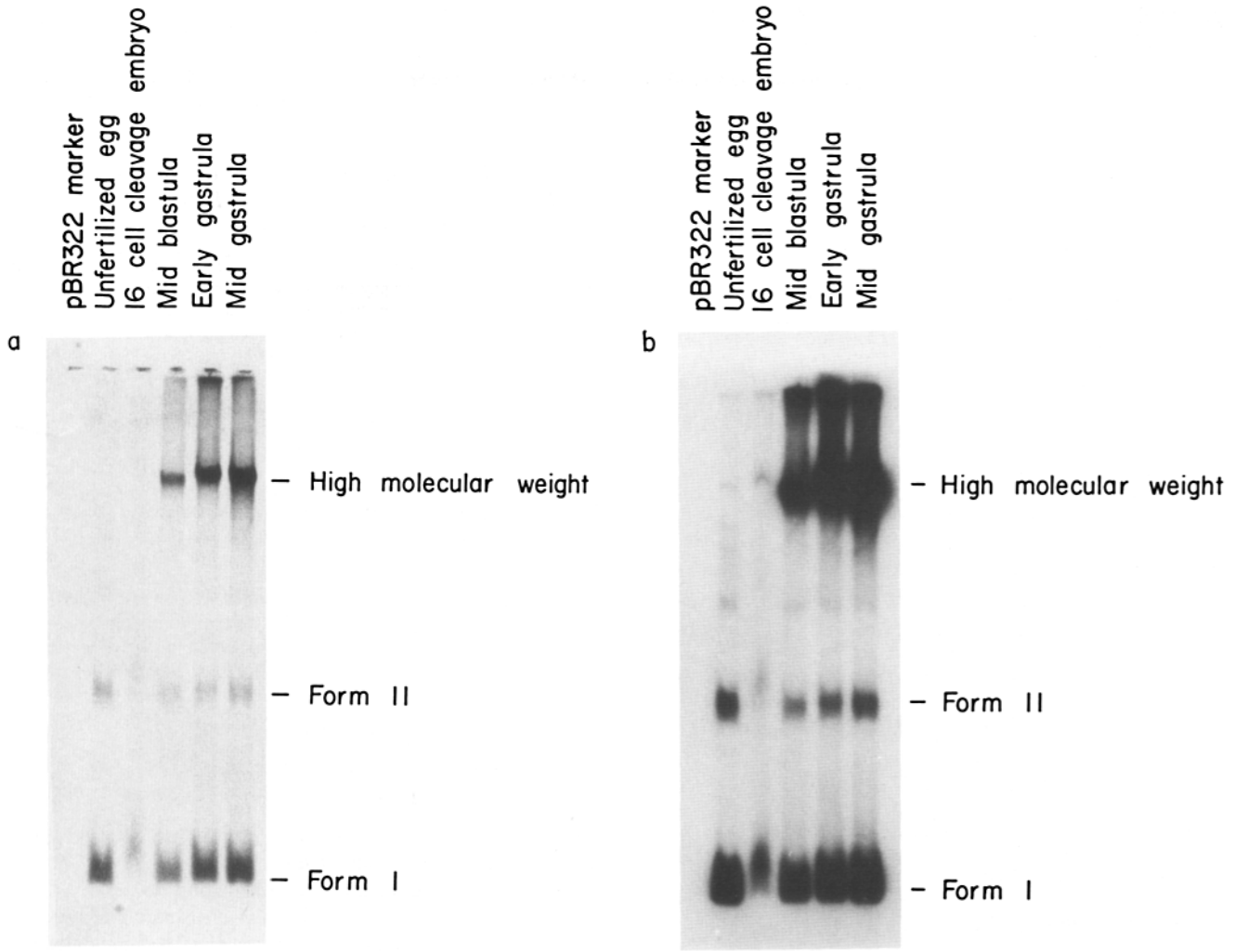

Figure 1. Incorporation of biotinylated nucleotides into pBR322 plasmid and endogenous high molecular weight DNA in vivo. (*a*) 4 ng pBR322 Form I DNA, 0.05 μCi [^{32}P]TTP, 10 pmol bio-11-dCTP, and 10 pmol bio-11-dUTP were coinjected into either unfertilized eggs or embryos at the 1–2-cell stage. DNA was isolated after 4 h from the unfertilized eggs and after 2.75, 6.0, 8.0, and 9.0 h from the embryos. DNA was isolated and subjected to electrophoresis on 1% agarose gels as described in Materials and Methods. Each lane was loaded with DNA from 5 eggs. After electrophoresis, the DNA was transferred to nitrocellulose filters using the Southern procedure. The incorporated biotinylated nucleotides were detected using the Detek-hrp streptavidin–horseradish peroxidase nucleic acid detection system. Lane *1* contains pBR322 marker DNA, which is not visualized by the detection system. Staining conditions were chosen such that the Form I, Form II, and high molecular weight bands were clearly defined at later stages of embryogenesis. As a result synthesis at the 16-cell stage was not prominently stained. Using more sensitive detection conditions, synthesis at the 16-cell stage can be emphasized, but lanes *5* and *6* become overstained, obscuring the bands (not shown). (*b*) An autoradiogram of the same gel shown in *a*. Synthesis at the 16-cell stage is more visible here than in *a*.

and without grossly modifying the apparently normal replication of either the endogenous or the microinjected DNA molecules.

Biotinylated Nucleotides were Incorporated in Proportion to Their Representation in the Endogenous Deoxynucleoside Triphosphate Pools

The internal deoxynucleoside triphosphate pools in *Xenopus laevis* eggs have been determined by Woodland and Pestell (43) to be 13, 16, 11, and 9 pmol each for dATP, dCTP, dGTP, and TTP, respectively. We microinjected biotinylated nucleoside triphosphates in amounts ranging from ~3% (Fig. 3, lane *1*) to slightly in excess of 100% (Fig. 3, lane *5*) of the endogenous pools. Incorporation increased in proportion to the amounts injected up to at least 3 pmol of each nucleoside triphosphate analog per egg. As greater amounts of biotinylated nucleoside triphosphates were microinjected, the mobility of the biotinylated DNA molecules in the gel decreased (Fig. 3, lane *5* especially), presumably because the increased bulk of the newly synthesized DNA retarded its migration (see Fig. 9 and Discussion). It is important to emphasize that synthesis of φX174 DNA appeared to be normal even when the amounts of biotinylated nucleoside triphosphates microinjected exceeded the endogenous dNTP pools. We did note in other experiments, however, that survival of embryos microinjected with amounts of biotinylated nucleo-

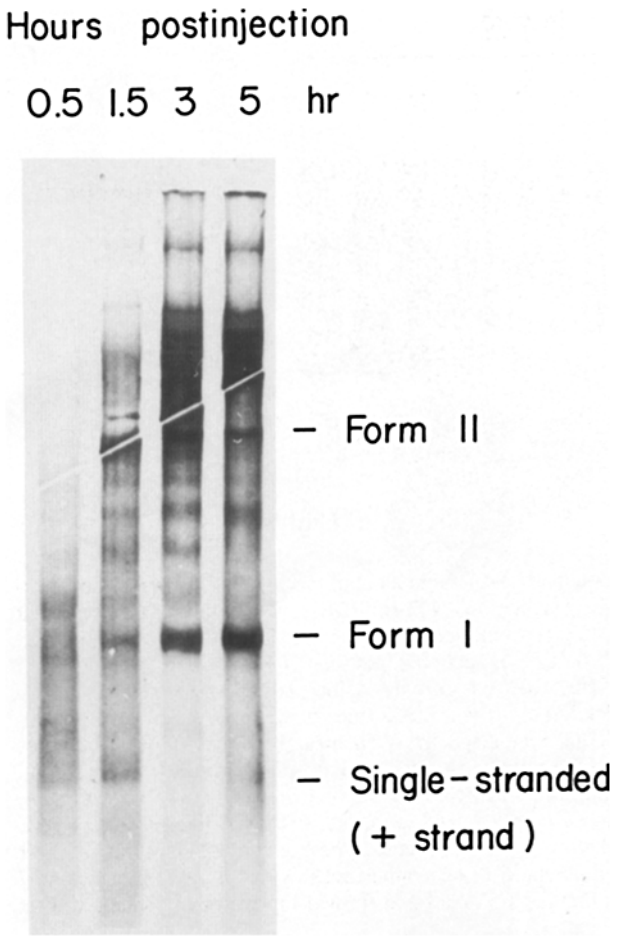

Figure 2. Incorporation of biotinylated nucleotides in vivo during conversion of microinjected single-stranded bacteriophage φX174(+) strand DNA to double-stranded Form I and Form II DNA molecules. 2 ng single-stranded φX174 DNA and 15 pmol each of bio-7-dATP, bio-11-dCTP, and bio-11-dUTP were coinjected into unfertilized eggs. DNA was subsequently isolated at the indicated times and subjected to electrophoresis as described in Fig. 1 *a*. Each lane was loaded with DNA from eight eggs. After Southern transfer, incorporated biotinylated nucleotides were visualized using the BluGENE streptavidin–alkaline phosphatase–based nonradioactive nucleic acid detection system.

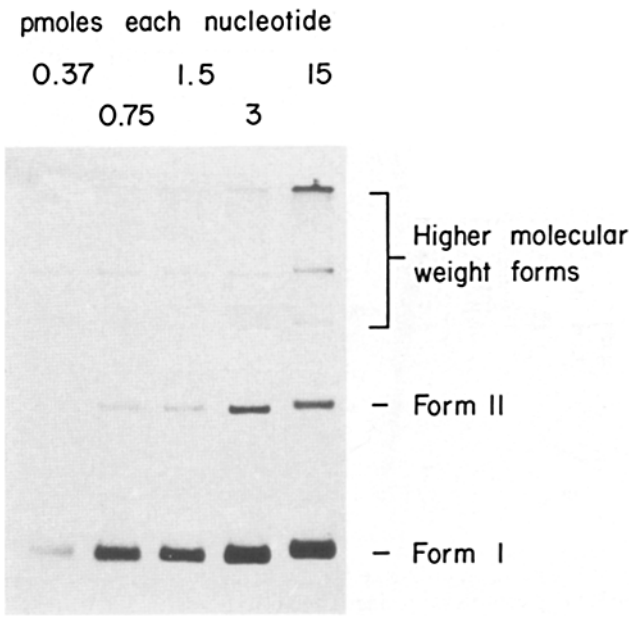

Figure 3. Amount of biotinylated nucleotide incorporated into newly synthesized DNA as a function of the amount injected into the eggs. 4 ng single-stranded φX174 DNA and the indicated amounts of bio-7-dATP, bio-11-dCTP, and bio-11-dUTP were microinjected into unfertilized eggs. After 4 h DNA was isolated and analyzed as in Fig. 2. Each lane was loaded with DNA from five eggs.

side triphosphates greater than the endogenous pools was markedly decreased by the time of neurulation.

Quantitation of the Efficiency of Incorporation of Biotinylated Nucleotides In Vivo

To quantitate the efficiency of incorporation of biotinylated nucleotides, we compared the amount of biotinylated nucleotides incorporated in a defined in vitro reaction from which the unbiotinylated homologue had been omitted vs. the amount incorporated using the same template in vivo. Synthesis in vitro was carried out using primed single-stranded φX174(+) strand DNA and the Klenow fragment of *E. coli* DNA polymerase I in a reaction from which TTP was omitted and replaced entirely by bio-11-dUTP (see Materials and Methods). The newly synthesized strands of the fully double-stranded Form II DNA molecules, which migrated as a discrete band on an agarose gel, were ~24% biotinylated (i.e., all dTMPs were replaced by bio-dUMPs).

The amount of incorporated biotinylated nucleotides detected using the BluGENE (Bethesda Research Laboratories) kit on known (ethidium bromide–stained bands compared to a titration of DNA of known concentration) amounts of DNA synthesized in vitro was then visually compared to the amount detected on DNA synthesized in microinjected eggs in vivo (Fig. 4). 15 pmol each of bio-7-dATP, bio-11-dCTP, and bio-11-dUTP were microinjected in the in vivo experiment.

To quantitate the efficiency of incorporation we assumed that both strands of the Form II DNA synthesized in vivo were biotinylated. This could lead to an underestimate of the efficiency of biotinylation for those molecules in which only one strand had been synthesized in vivo. Thus, our calculation of the efficiency of incorporation could be low by a factor approaching two. We also assumed that all three biotinylated nucleoside triphosphates were incorporated at similar efficiencies (i.e., that bio-11-dCTP substituted for dCTP and bio-7-dATP for dATP with at least the same efficiency that bio-11-dUTP substituted for TTP).

Fortuitously, comparable amounts of Form II DNA (monitored by ethidium bromide staining) synthesized in vivo and in vitro exhibited comparable staining for biotinylated nucleotides (legend to Fig. 4). We therefore calculated the efficiency of incorporation of biotinylated nucleotides in vivo to be at least one-sixth of the unbiotinylated (endogenous) nucleotide incorporation rate. This rate is based on the presumption that the DNA synthesized in vitro contained only one strand synthesized with only one biotinylated nucleoside triphosphate precursor, whereas the DNA syn-

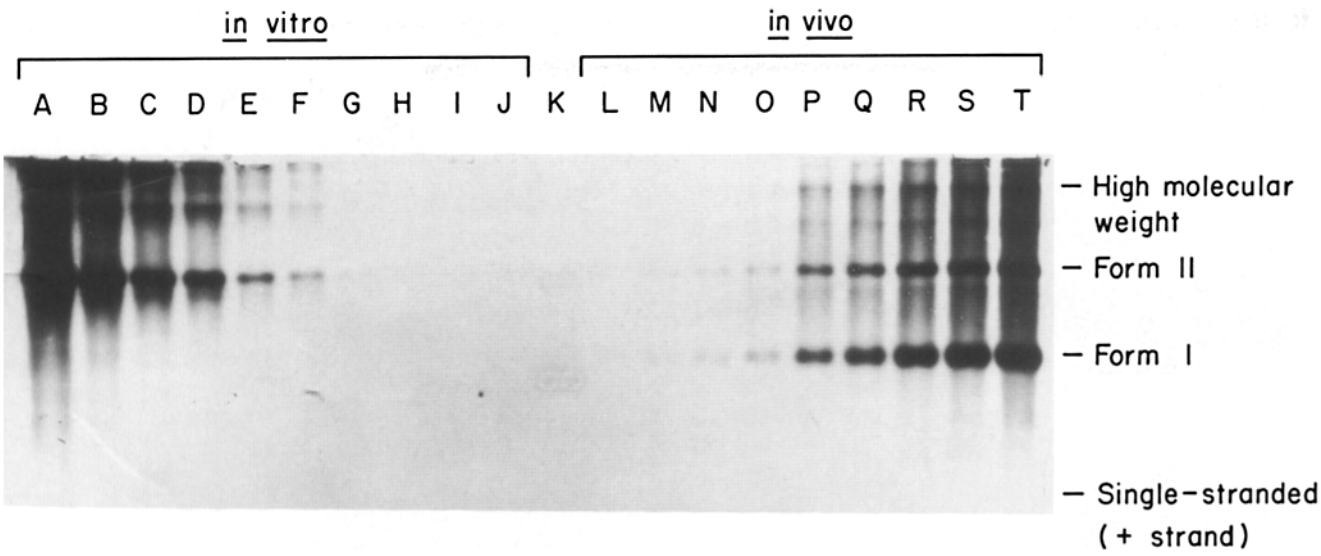

Figure 4. Quantitation of the efficiency of incorporation of biotinylated nucleotides in vivo. The amount of biotinylated nucleotide incorporated during conversion of single-stranded bacteriophage φX174 DNA to double-stranded φX174 Form II DNA was compared to the amount incorporated into Form II DNA in vivo. Lanes *A–J* contain dilutions of the reaction product synthesized in vitro. Lane *K* is an unbiotinylated φX174 marker. Lanes *L–T* contain dilutions of the product synthesized in vivo using the reaction conditions in Fig. 3, lane *5*. The amount of Form II DNA in each lane was quantitated by comparing the intensity of the ethidium bromide-stained DNA band to that of a band of known concentration run in an adjacent lane. The amounts of Form II added in lanes *A–T* are as follows: 30, 8, 3, 1.5, 0.3, 0.15, 0.03, 0.015, 0.007, 0.0035, 200 (standard), 0.06, 0.012, 0.025, 0.05, 0.25, 0.5, 1.25, 2.5, and 5 ng, respectively. Incorporated biotinylated nucleotides were visualized with the BluGENE detection system. (Only relative amounts of incorporated biotinylated nucleotides in each Form II band were compared visually. Form I DNA is not made in vitro and therefore can not be compared to Form I made in vivo.) For example, the Form II band in lane *G* (0.03 ng synthesized in vitro) is less intensely stained than the band in lane *N* (0.025 ng synthesized in vivo). Since the DNA in lane *G* was 24% biotinylated on one strand (12% if both strands are considered), the Form II DNA in lane *N* must have incorporated >12% biotinylated nucleotides. Similarly, the Form II band in lane *C* (3 ng synthesized in vitro) is as intensely stained as the Form II band in lane *S* (2.5 ng synthesized in vivo), again indicating that the Form II band formed in vivo must contain at least 12% biotinylated nucleotides.

thesized in vivo could contain up to two strands each synthesized with three biotinylated nucleoside triphosphates. This suggests that a minimum of 16.7% × 3/4 = 12%, or one out of every eight nucleotides incorporated in vivo was biotinylated.

Stability of Heavily Biotinylated DNA In Vivo

Heavily biotinylated DNA (every TTP on one strand replaced with a biotinylated dUTP) might be expected (see Discussion) to be subject to extensive repair processes in unfertilized eggs and embryos. To test this hypothesis, biotinylated φX174 Form II DNA synthesized in vitro (see Materials and Methods) was microinjected into unfertilized *Xenopus laevis* eggs along with [^{32}P]dATP. As shown in Fig. 5 *a*, microinjected biotinylated Form II DNA was not degraded for at least 2 h in the eggs. Instead, the heavily biotinylated Form II DNA was efficiently converted to Form I (supercoiled) DNA and to higher molecular weight forms, as is unbiotinylated DNA (7, 8, 17, 39). Identical results were obtained in microinjected embryos (Fig. 1 and unpublished observations). As shown in Fig. 5 *b* for unfertilized eggs and Fig. 1 *b* for embryos, incorporation of [^{32}P]dATP was into the same plasmid forms with similar kinetics. 5 h after microinjection, a small decrease in biotinylated DNA perhaps may have occurred in both the unfertilized eggs (Fig. 5 *a*) and embryos (not shown). This may not be a physiological repair process, since some of the microinjected unfertilized eggs and embryos also become necrotic around this time. We conclude, therefore, that even heavily biotinylated DNA is sufficiently stable to persist, undegraded, in unfertilized eggs and in developing *Xenopus laevis* embryos for at least several hours. The biotinylated DNA cannot, therefore, be subject to extensive DNA repair during this time period. We also conclude that the parental (biotinylated) and newly synthesized daughter (^{32}P-labeled) strands are converted to the same forms with similar kinetics.

Electron Microscopic Visualization of Incorporated Biotinylated Nucleotides by Streptavidin–Colloidal Gold and Streptavidin–Ferritin Conjugates

To visualize the sites of incorporation of biotinylated nucleotides, DNA isolated either from in vitro reactions or from in vivo synthesis was incubated with streptavidin–colloidal gold or streptavidin–ferritin conjugates. The DNA was spread for electron microscopy using either the microdrop procedure (28) or Kleinschmidt spreading procedure as modified by Davis et al. (15). To demonstrate the specificity of incorporation, Hind III restriction fragments of pX108 were digested briefly with exonuclease III, then end-labeled by fill-in synthesis using Klenow fragment with bio-11-dUTP substituted for TTP. As shown in Fig. 6 *a*, the streptavidin–colloidal gold conjugate specifically labeled the ends of the restriction fragments. No colloidal gold particles were

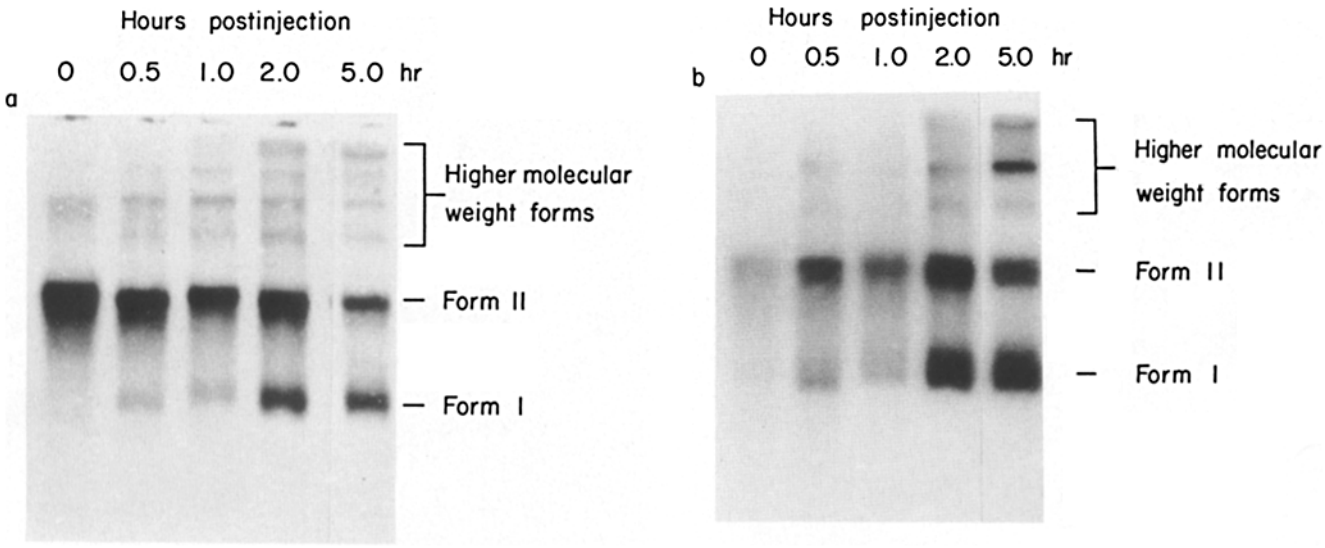

Figure 5. Stability of microinjected biotinylated double-stranded DNA in vivo. (*a*) Biotinylated φX174 Form II DNA (24% bio-11-dUTP in [−] strand) was synthesized in vitro as described in Materials and Methods. 2 ng of this DNA was microinjected into unfertilized *Xenopus laevis* eggs along with [^{32}P]dATP to monitor replication. At the indicated times, DNA was reisolated and analyzed as described in the legend to Fig. 2. DNA extracted from 5 eggs was applied to each lane. The amount of biotinylated DNA in the various forms at 2 h postinjection (as monitored using the nonradioactive nucleic acid detection kit BluGENE) was equal, within measurement error, to the amount in Form II DNA at 0 h. Conversion to biotinylated Form I DNA was observed by 2 h postinjection. (*b*) An autoradiogram of the same gel as in Fig. 5 *a*. The small amount of incorporation at 0 h post injection results from a small amount of synthesis that occurs during the time it takes to microinject a series of unfertilized eggs and transfer them to 0°C.

observed at internal locations within the restriction fragment or associated with unbiotinylated plasmid DNA molecules included as a control in the spreading mixture.

Similar binding specificity to biotinylated DNA was observed when an entire molecule contained biotinylated nucleotides. Complementary strands to φX174(+) strand DNA were synthesized using bio-11-dUTP to replace the TTP in an in vitro reaction as described in Materials and Methods. The biotinylated double-stranded φX174 Form II DNA was mixed with unbiotinylated double-stranded pXGαβ1 DNA (17 kb) then reacted with streptavidin–colloidal gold and prepared for electron microscopy. Fig. 6 *b* shows that the biotinylated φX174 DNA was specifically associated with streptavidin–colloidal gold, whereas little or no gold was associated with the control unbiotinylated pXGαβ1 DNA. It was also clear, however, that binding of the streptavidin–colloidal gold interfered with the proper spreading of the DNA molecules. In part, these difficulties were due to the size and high density of the gold particles. In addition, all commercially available streptavidin–gold conjugates have a large number of potential biotin binding sites (for example, ~64 potential sites on a 20-nm gold particle). This apparently caused both inter- and intrastrand cross-linking of the biotinylated DNA molecules. To reduce the cross-linking, titration of the streptavidin–colloidal gold with free biotin was carried out before the binding reaction. The binding of streptavidin–colloidal gold to biotinylated φX174 DNA before and after complete titration of the biotin binding sites is shown in Fig. 7, *a* and *b*. None of the gold particles were able to bind the biotinylated DNA in the latter case. This demonstrates that the streptavidin–colloidal gold binds to biotin moieties attached to the DNA. In contrast, untitrated particles caused clumping (Fig. 7 *a*) and extensive cross-linking of the biotinylated DNA (Fig. 7 *c*). We then attempted to reduce the number of potential binding sites per gold particle to an average of one. Biotinylated φX174 circular and linear DNA molecules after reacting with titrated streptavidin–colloidal gold conjugates (20-nm size) are shown in Fig. 8, *a* and *b*. Fig. 8 *c* shows the association of streptavidin–colloidal gold particles (20 nm) with long linear DNA molecules gap-filled with biotinylated nucleotides. A higher magnification electron micrograph of a heavily biotinylated small fragment associated with closely spaced streptavidin–colloidal gold conjugates (20-nm size) is shown in Fig. 8 *d*. The closest spacing between the colloidal gold particles on this fragment is ~50 bp, approaching the theoretical limit for a 20-nm particle. Since the gold particles apparently impeded spreading (i.e., long fragments labeled heavily with 20-nm gold particles, as in Fig. 8 *d*, do not spread well) we tested streptavidin–colloidal gold conjugates of smaller size (5 nm) as well as streptavidin–ferritin conjugates (5–7 nm). Fig. 8 *e* shows the association of streptavidin–ferritin conjugates with biotinylated DNA. Although the contrast of the bound streptavidin–ferritin conjugates was not as striking as with the 20-nm colloidal gold particles, they could still be distinctly visualized. Moreover, the smaller particles allowed better spreading of the DNA, especially with longer molecules. Further experiments are in progress to increase the contrast and decrease the background using streptavidin–ferritin conjugates; these conjugates have a potential resolution of 10–15 bp.

Discussion

In this paper we describe a method for visualizing nascent DNA synthesized in vivo. It is important to emphasize that

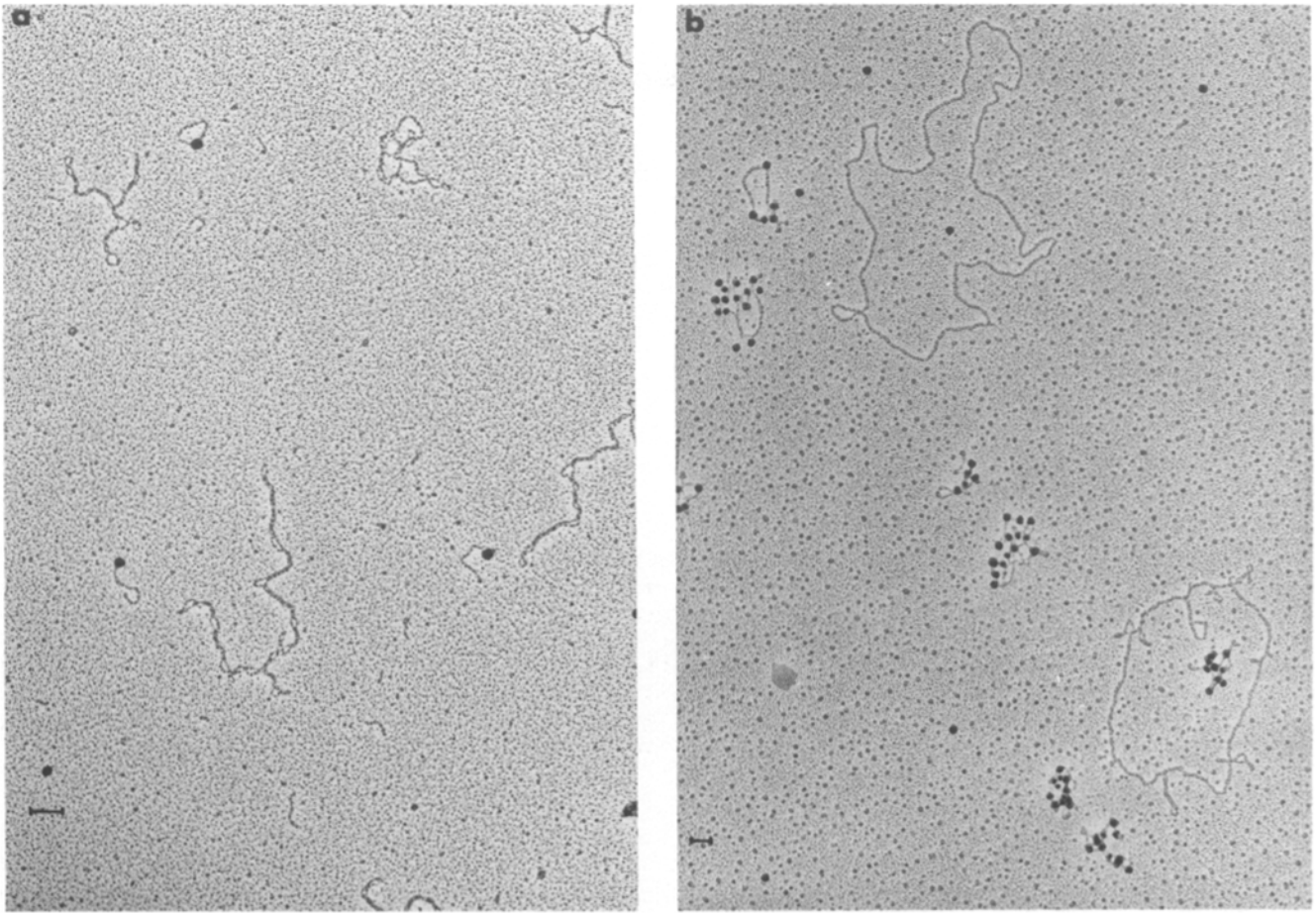

Figure 6. Electron microscopic visualization of specific binding of streptavidin–colloidal gold conjugate (20-nm size) to biotinylated DNA. (*a*) End-labeled restriction fragments. Hind III–digested pX108 plasmid DNA was biotinylated as described in Materials and Methods. The biotinylated DNA fragments were mixed with unbiotinylated supercoiled plasmid DNA and labeled with colloidal gold conjugate, spread by the droplet procedure, picked up on glow-discharged carbon grids, and processed for electron microscopy. Colloidal gold was found specifically associated with the ends of the restriction fragments only. (*b*) Uniformly labeled φX174 DNA. Biotinylated φX174 DNA was prepared as described in Materials and Methods. A mixture of biotinylated φX174 DNA (5.4 kb) along with unbiotinylated pXGαβ1 DNA (17 kb) was labeled with streptavidin–colloidal gold conjugate, spread for electron microscopy under aqueous conditions, and photographed on a Zeiss EM 109 microscope. Colloidal gold conjugate was observed exclusively associated with 5.4 kb φX174 biotinylated DNA, but the DNA is clumped and cross-linked. Bars, 0.1 μm.

this method faithfully monitors the apparently normal incorporation of nucleoside triphosphates into chromosomal DNA during early embryogenesis, and can be used to analyze physiological replication processes. The method exploits both the high affinity of streptavidin for biotin and the high electron density of gold and ferritin particles. Avidin, a 68,000 D glycoprotein from the eggwhite (20), and streptavidin, a protein secreted by *Streptomyces avidinii* (14), both exhibit very high affinity for biotin ($K_d = 10^{-15}$ M). This property has been used in the development of a variety of immunobiochemical and immunoelectron microscopic techniques. For example, avidin–ferritin conjugates have been used earlier to detect, by electron microscopy, discontinuities and repair sites in linear DNAs labeled in vitro with bio-11-dUTP (26, 34). The use of avidin in sensitive detection experiments, however, has some critical limitations. Since avidin is positively charged, with pI = 10 at pH 7, it tends to bind nonspecifically to negatively charged molecules like nucleic acids (our unpublished observations). In addition, the glycoprotein moiety of avidin tends to bind to a variety of carbohydrates and lectins, which causes high backgrounds (our unpublished observations). Substitution of streptavidin, which has pI = 5 at physiological pH, for avidin, seemed to solve both the nonspecific binding and high background problems.

Use of biotinylated nucleoside triphosphate analogs by DNA polymerases in DNA synthesis has been demonstrated previously in vitro (29) and in crude nuclear extracts (9, 10). In this study we show that replicating endogenous chromosomal DNA as well as replicating exogenous DNA microinjected into *Xenopus laevis* eggs or embryos were efficiently labeled in vivo with biotinylated analogs of the normal precursors of DNA synthesis. The rate of incorporation of these analogs into DNA was increased proportionally by increasing the concentration of the microinjected biotinylated dNTP pools inside the unfertilized or fertilized eggs. This

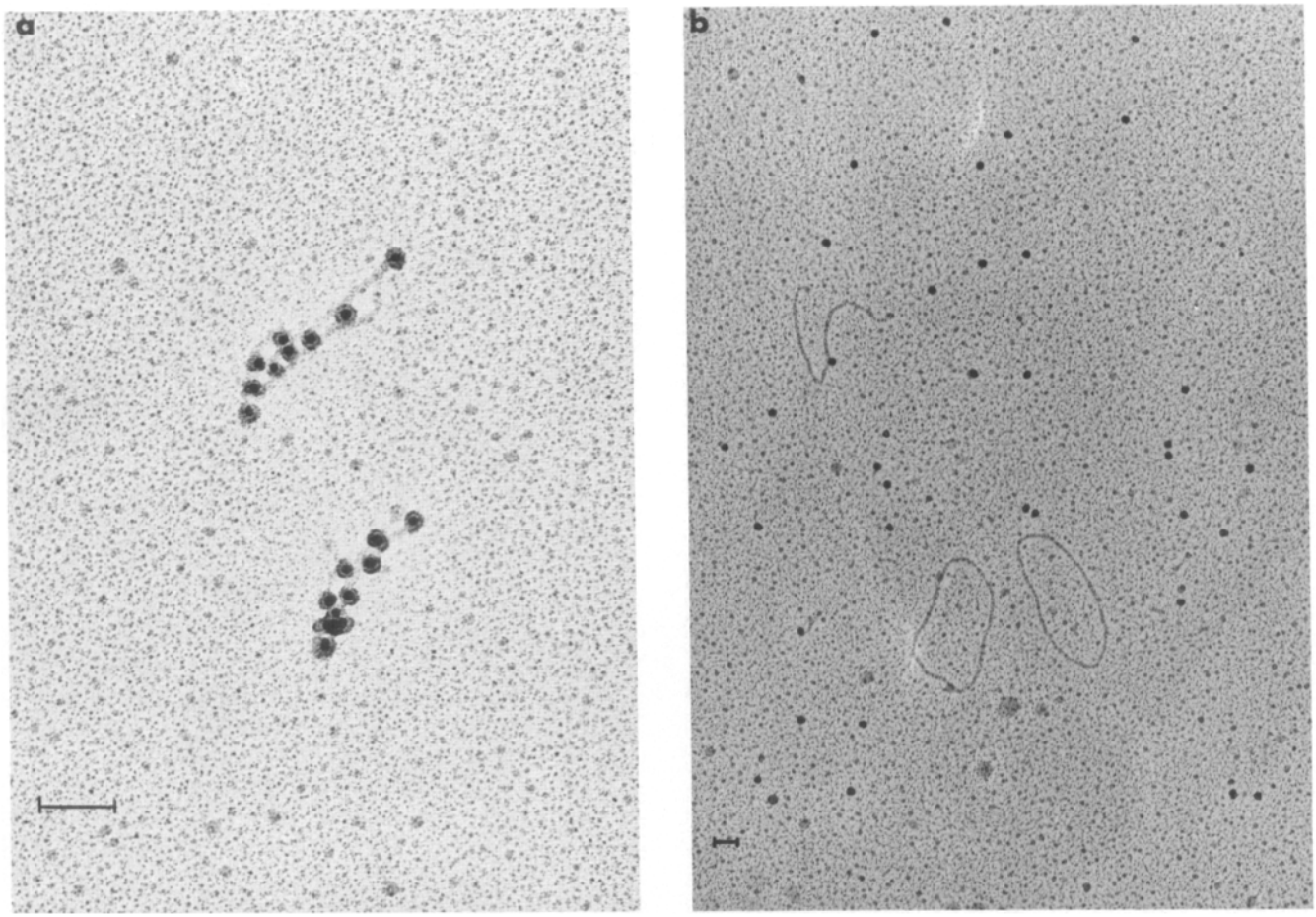

Figure 7. Biotin titration of streptavidin-colloidal gold and its effect on binding. Streptavidin-colloidal gold conjugate (20-nm size) was titrated with d-biotin to different extents (0–100%) and reacted with the in vitro–synthesized biotinylated φX174 DNA. The DNA was spread under aqueous conditions as described earlier. (*a*) Without any biotin. (*b*) Titrated with excess biotin. (*c* [next page]) Cross-linking of the biotinylated DNA by untitrated multivalent streptavidin–colloidal gold. Note that the colloidal gold is almost invariably associated with crossover nodes.

suggests that the analogs successfully compete with the normal nucleoside triphosphates as substrates for DNA polymerases in vivo, in spite of the projecting biotin side chains that might be expected to interfere with incorporation (Fig. 9). Moreover, the kinetics of incorporation exactly paralleled the incorporation of unbiotinylated radioactive nucleotides in the same eggs and embryos (Fig. 1 *b*). The biotin-containing side chains significantly affect the bulk of the DNA molecule; this is suggested by the decreased mobility observed for heavily biotinylated DNA on agarose gels (Fig. 3, lane *5*). This alteration apparently does not significantly perturb normal DNA replication.

The amount of biotinylation was proportional to the amounts of the biotinylated nucleoside triphosphates injected (Fig. 3). Incorporation of the biotinylated nucleoside triphosphates could be as high as 12% (1 in 8) of the total nucleotides incorporated. Both the endogenous chromosomal DNA and the microinjected exogenous DNA underwent multiple rounds of DNA replication. The biotinylated plasmid DNA accumulated linearly over time (based on densitometric scans of the bands in Fig. 1 *a* and in similar experiments), whereas the biotinylated high molecular weight DNA accumulated exponentially. This accumulation paralleled the accumulation of radioactive dNTPs in the same embryos. Moreover, the embryos underwent normal divisions at least until the late blastula or early gastrula stages, and apparently developed normally.

The incorporation levels of the analogs relative to normal substrates was somewhat lower in vivo than the 30–40% efficiency reported in vitro (29). Moreover, incorporation into endogenous high molecular weight DNA was much more efficient than into microinjected plasmid DNA (Fig. 1 *a*). The reason for this greater efficiency is not entirely clear. It is not related to the incorporation of biotinylated precursors of DNA synthesis, since Marini et al. (33) have similarly shown in incorporation experiments that high molecular weight DNA is replicated much more efficiently than circular plasmid DNA microinjected into the embryos (also see Fig. 1 *b*). The greater efficiency of replication of high molecular weight DNA does not simply result from the fact that chromosomal DNA is found in the nucleus. Forbes et al. (18), Lohka and Masui (31), and Newport (37) have shown that microinjected plasmid DNA is rapidly assembled into structures that are morphologically and functionally indis-

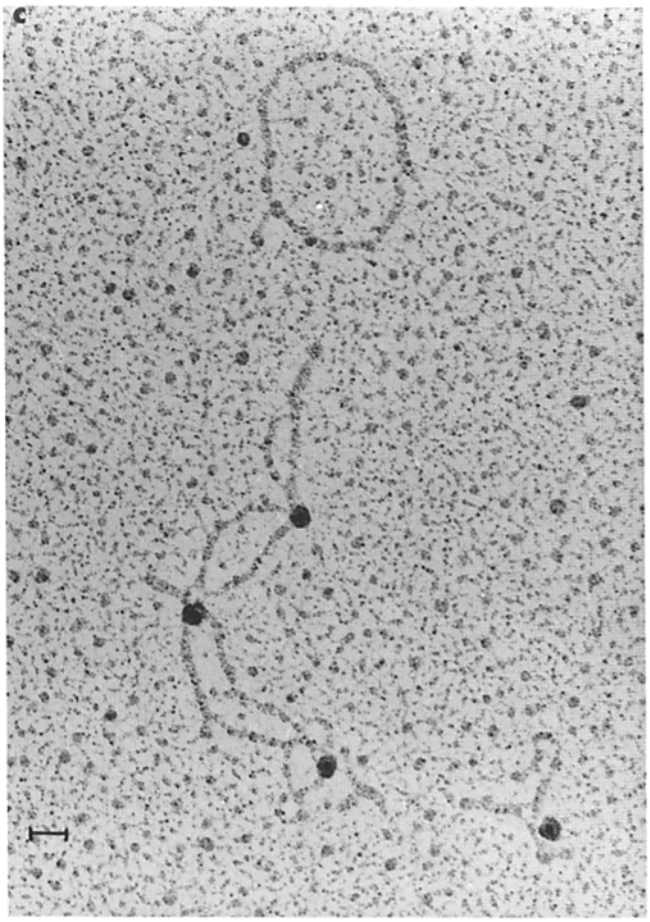

tinguishable from normal nuclei. Moreover, formation of a nuclear envelope around the microinjected DNA was essential for efficient replication to occur (37).

To see whether the biotinylated nucleotides incorporated into the DNA were excised or repaired we microinjected heavily biotinylated circular DNA. Repair might have been expected a priori based on the structure of biotinylated DNA, since the biotin-containing side chain (11 atom linker) projects ~21–22 Å out of the major grove of the helix (Fig. 9). These biotins are readily accessible to binding of the electron-dense ligands, and are thus presumably also "visible" to repair enzymes. Heavily biotinylated DNA was nonetheless stable for at least the first 4–5 h after microinjection into either unfertilized eggs or embryos. This suggests that there are no repair mechanisms that quickly eliminate or repair the biotinylated nucleotides during early embryogenesis. We do not rule out the possibility that repair mechanisms work slowly or, alternatively, may be lacking in early embryogenesis.

We also observed that the nicked circular biotinylated DNA underwent normal conformational changes into supercoiled DNA. The microinjected heavily biotinylated DNA also underwent efficient replication as indicated by the incorporation of radiolabeled nucleotides (Fig. 5 *b*). We conclude that biotinylated nucleotides can be incorporated efficiently into nascent DNA, are quite stable in early embryos, do not serve as barriers to the synthesis of complementary strands, and do not prevent ligation and torsional stress. The above observations imply that biotinylated nucleotides can be used successfully to study normal replication processes in vivo, both for pulse labeling and for some continuous labeling experiments.

Biotinylation is particularly suitable for studying DNA replication in vivo, because the nascent DNA can be visualized directly both on agarose gels and by electron microscopy. Streptavidin–gold or streptavidin–ferritin conjugates bind efficiently and specifically to the biotinylated portions of the DNA. There is little or no nonspecific binding (Fig. 6). Cross-linking and high backgrounds are eliminated or considerably reduced by the judicious use of biotin-titrated conjugates (Figs. 7 and 8). Our results also show that, although the 20-nm particles gave the highest contrast, smaller particle sizes were more useful for resolving sites of nascent DNA synthesis. Moreover, the large particles impeded spreading of the long molecules of DNA.

The potential resolution of the technique using streptavidin–colloidal gold or streptavidin–ferritin conjugates is such that individual Okazaki fragments (~200 bp) can be identified easily. Two adjacent gold particles with associated streptavidin moieties could theoretically be located at two sites out of phase by 180° and translated along the helical axis by 17.5 Å (Fig. 9). Depending on the size of the gold particle the resolution would be 13, 26, or 50 bp (for 5-, 10-, or 20-nm particles, respectively). In practice, however, technical difficulties involved in spreading dense particle–bound DNA for electron microscopy presumably set a lower limit to the resolution of the method.

The mechanism of chromosomal DNA replication (11–13) in higher eukaryotes has proven elusive (3, 5, 6) during the 35 years since the essential features of duplex DNA replication were first set forth (40). Recently, we have postulated that separation of the strands of the double helix during chromosomal DNA replication in embryos of the frog, *Xenopus laevis* is temporally and spatially uncoupled from synthesis of the daughter strands (2, 4, 19). The strand separation hypothesis (19) has been proposed also as a possible replication mechanism in human melanoma cells (31a). To distinguish between replication by the strand separation mechanism and replication at processive replication forks we developed the high resolution method presented in this paper to localize sites of nascent DNA synthesis on chromosomal DNA. This method should prove useful also for studying the temporal and spatial relationships of sites of nascent DNA synthesis relative to other cellular processes including, among many others, gene expression and chromatin assembly.

We thank Nicholas Marini for purifying the PXGαβ1 marker DNA sample; Dr. Gautam Gupta for the computer graphics; Deborah Stowers and Jenny Keim for excellent technical assistance; and Howard Kaiserman, Diny Poll, Charisse Buising, and Michelle Gaudette for critical discussions. We are grateful to Mary Nims for her assistance with the preparation of the manuscript.

This research was supported by grants from the National Science Foundation, the National Institutes of Health, and the Iowa State University Office of Biotechnology.

Received for publication 6 November 1987, and in revised form 22 March 1988.

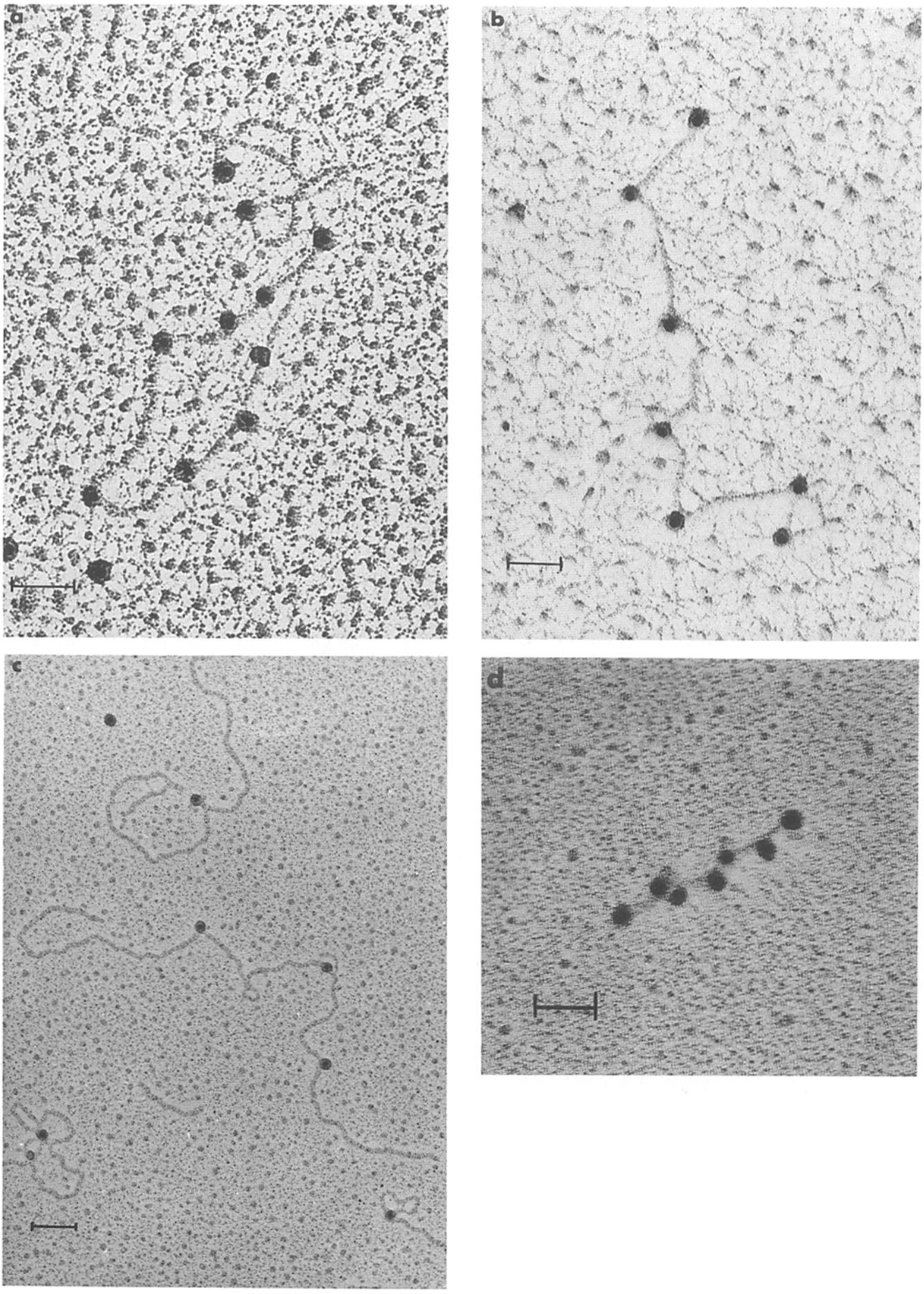
a
b
c
d

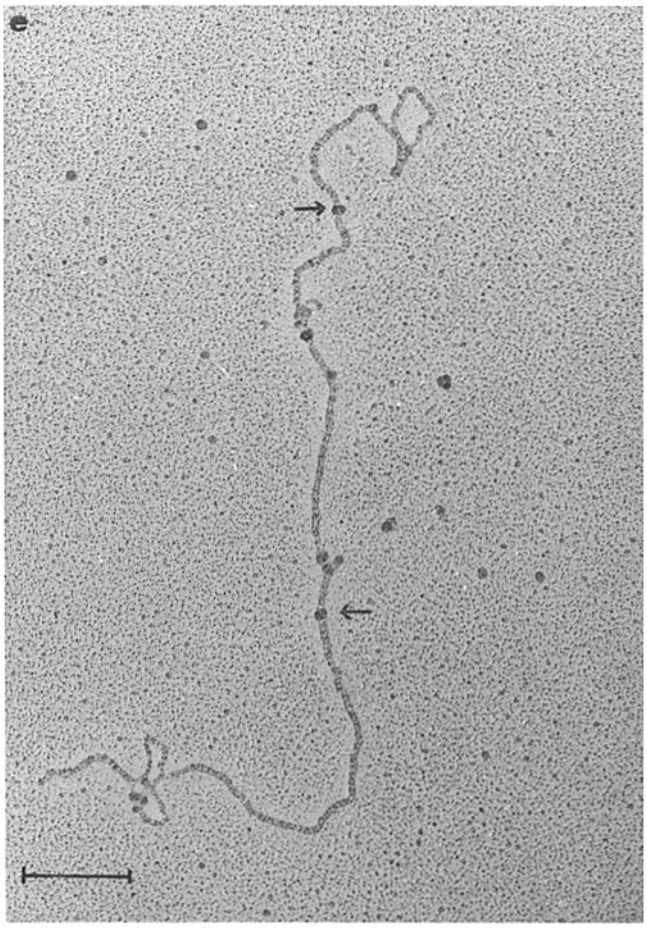

Figure 8. Streptavidin–colloidal gold conjugate (20-nm size) binding to biotinylated DNA. Streptavidin–colloidal gold was titrated with biotin to optimize binding while minimizing cross-linking and heavy backgrounds. (*a*) In vitro–biotinylated φX174 Form II DNA. (*b*) Linearized biotinylated φX174 DNA. (*c*) In vitro–biotinylated nicked long linear calf thymus DNA labeled with 20-nm colloidal gold. This DNA was relatively sparsely labeled (by nick translation). (*d*) A short fragment (~1 kb) of heavily biotinylated φX174 DNA reacted with the streptavidin–colloidal gold conjugate. Longer molecules of heavily biotinylated DNA reacted with 20-nm colloidal gold particles do not spread well. (*e*) DNA as in *c*, but labeled with streptavidin–ferritin conjugate. Note that binding of ferritin particles does not induce kinks on the spread DNA, unlike the more dense gold particles (*b* especially).

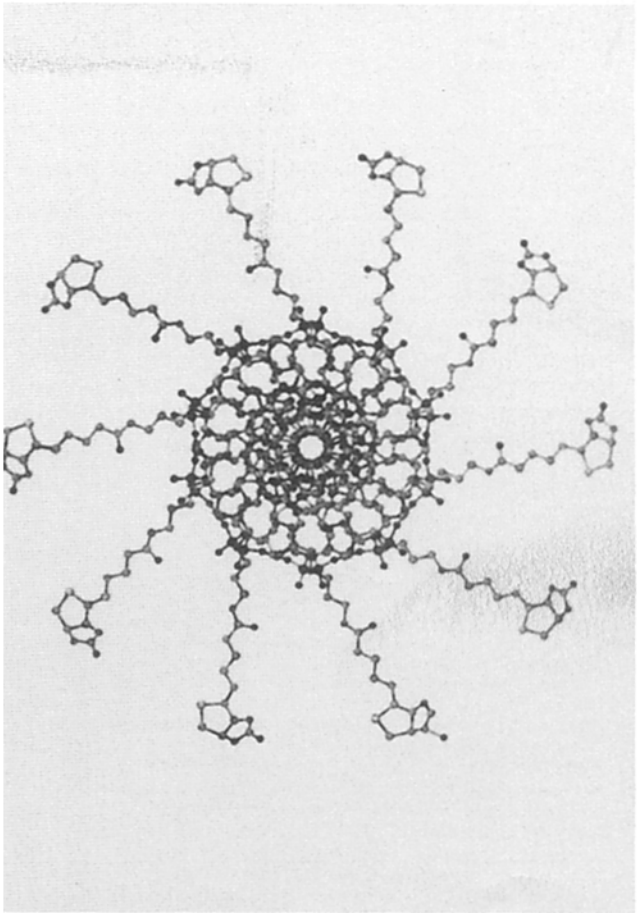

Figure 9. Computer projection of a representative model of bio-11-dUTP substituted poly(dA)–poly(dU). The figure represents the DNA helix viewed down the helical axis. One turn of the B-DNA duplex with biotin labeled at 5-position on U; the length of the biotin-11 atom linker is ~21–22 Å. Theoretically two gold particles (10–20 nm) with the associated streptavidin moieties could be located at two sites out of phase by 180° and translated along the helical axis by 17.5 Å. Binding of one gold particle (10–20 nm) may protect in principle the whole length of such a segment and stereochemically prevent binding similar particles at many of the available adjacent binding sites. This puts a theoretical constraint on the number of particles that could bind to a certain length of DNA, even though potentially DNA may be biotinylated every eight nucleotides.

References

1. Becker, C. R., J. W. Efcavitch, C. R. Heiner, and N. F. Kaiser. 1985. Use of a C4 column for reversed phase high performance liquid chromatographic purification of synthetic oligonucleotides. *J. Chromatogr.* 326: 293–299.
2. Benbow, R. M. 1985. Activation of DNA synthesis during early embryogenesis. *In* Biology of Fertilization. Vol. 3. C. B. Metz and A. Monroy, editors. Academic Press Inc., New York. 299–345.
3. Benbow, R. M., and C. C. Ford. 1975. Cytoplasmic control of nuclear DNA synthesis during early development of *Xenopus laevis*: a cell free assay. *Proc. Natl. Acad. Sci. USA.* 72:2437–2441.
4. Benbow, R. M., M. F. Gaudette, P. J. Hines, and M. Shioda. 1985. Initiation of DNA replication in eukaryotes. *In* Control of Animal Proliferation. A. L. Boynton and H. L. Leffert, editors. Academic Press Inc., New York. 449–483.
5. Benbow, R. M., H. Joenje, S. H. White, C. B. Breaux, C. C. Ford, and R. A. Laskey. 1977. Cytoplasmic control of nuclear DNA replication in *Xenopus laevis*. *In* International Cell Biology 1976–1977. B. R. Brinkley and K. R. Porter, editors. The Rockefeller University Press, New York. 453–467.
6. Benbow, R. M., M. R. Krauss, and R. H. Reeder. 1978. DNA synthesis in a multienzyme system from *Xenopus laevis* eggs. *Cell.* 13:307–318.
7. Bendig, M. M. 1981. Persistence and expression of histone genes injected into *Xenopus* eggs in early development. *Nature (Lond.).* 292:65–67.
8. Bendig, M. M., and J. G. Williams. 1983. Replication and expression of *X. laevis* globin genes injected into fertilized *Xenopus* eggs. *Proc. Natl. Acad. Sci. USA.* 80:6197–6201.
9. Blow, J. J., and R. A. Laskey. 1986. Initiation of DNA replication in nuclei and purified DNA by a cell free extract of *Xenopus* eggs. *Cell.* 47: 577–587.
10. Blow, J. J., and J. V. Watson. 1987. Nuclei act as independent and integrated units of replication in a *Xenopus* cell-free DNA replication system. *EMBO (Eur. Mol. Biol. Organ.) J.* 6:1997–2002.
11. Callan, H. G. 1972. Replication of DNA in the chromosomes of eukaryotes. *Proc. R. Soc. Lond. B Biol. Sci.* 181:19–41.
12. Callan, H. G. 1973*a*. DNA replication in chromosomes of eukaryotes. *Cold Spring Harbor Symp. Quant. Biol.* 38:195–203.

13. Callan, H. G. 1973*b*. Replication of DNA in eukaryotic chromosomes. *Br. Med. Bull.* 29:192–215.
14. Chaiet, L., and F. S. Wolf. 1964. The properties of streptavidin, a biotin binding protein produced by *Streptomycetes*. *Arch. Biochem. Biophys.* 106:1–5.
15. Davis, R. W., M. Simon, and N. Davidson. 1971. Electron microscope heteroduplex methods for mapping regions of base sequence homology in nucleic acids. *Methods Enzymol.* 21D:413–428.
16. Edenberg, H. J., and J. A. Huberman. 1975. Eukaryotic chromosome replication. *Annu. Rev. Genet.* 9:245–284.
17. Etkin, L. D., and B. Pearman. 1987. Distribution, expression, and germ line transmission of exogenous DNA sequences following microinjection into *Xenopus laevis* eggs. *Development.* 99:15–23.
18. Forbes, D., M. Kirschner, and J. Newport. 1983. Spontaneous formation of nucleus-like structures around bacteriophage DNA microinjected into *Xenopus* eggs. *Cell.* 34:13–23.
19. Gaudette, M. F., and R. M. Benbow. 1986. Replication forks are underrepresented in chromosomal DNA of *Xenopus laevis* embryos. *Proc. Natl. Acad. Sci. USA.* 83:5953–5957.
20. Green, N. M. 1975. Avidin. *Adv. Protein Chem.* 29:85–133.
21. Guinta, D. R., J. Yun Tso, S. Narayanswamy, B. A. Hamkalo, and L. J. Korn. 1986. Early replication and expression of oocyte-type 5S RNA genes in a *Xenopus* somatic cell line carrying a translocation. *Proc. Natl. Acad. Sci. USA.* 83:5150–5154.
22. Gurdon, J. B. 1977. Methods for nuclear transplantation in Amphibia. *Methods Cell Biol.* 16:125–139.
23. Hand, R. 1978. Eukaryotic DNA: organization of the genome for replication. *Cell.* 15:317–325.
24. Huberman, J. A. 1968. Visualization of replicating mammalian and T_4 bacteriophage DNA. *Cold Spring Harbor Symp. Quant. Biol.* 33:509–524.
25. Huberman, J. A., and A. D. Riggs. 1968. On the mechanism of DNA replication in mammalian chromosomes. *J. Mol. Biol.* 32:327–341.
26. Hunting, D. J., S. L. Dresler, and G. de Murcia. 1985. Incorporation of biotin-labeled deoxyuridine triphosphate into DNA during excision repair and electron microscopic visualization of repair patches. *Biochemistry.* 24:5729–5734.
27. Kleinschmidt, A. K. 1968. Monolayer techniques in electron microscopy of nucleic acid molecules. *Methods Enzymol.* XII B:361–377.
28. Lang, D., and M. Mitani. 1970. Simplified quantitative electron microscopy of biopolymers. *Biopolymers.* 9:373–379.
29. Langer, P. R., A. A. Waldrop, and D. C. Ward. 1981. Enzymatic synthesis of biotin-labeled polynucleotides: novel nucleic acid affinity probes. *Proc. Natl. Acad. Sci. USA.* 78:6633–6637.
30. Leary, J. J., D. J. Brigati, and D. G. Ward. 1983. Rapid and sensitive colorimetric method for visualizing biotin-labeled DNA probes hybridized to DNA or RNA immobilized on nitrocellulose: bio-blots. *Proc. Natl. Acad. Sci. USA.* 80:4045–4049.
31. Lohka, M. J., and Y. Masui. 1983. Formation *in vitro* of sperm pronuclei and mitotic chromosomes induced by amphibian ooplasmic components. *Science (Wash. DC).* 220:719–721.
31a. Lönn, U., and S. Lönn. 1988. Extensive regions of single-stranded DNA in aphidicolin-treated melanoma cells. *Biochemistry.* 27:566–570.
32. Maniatis, T., E. F. Fritsch, and J. Sambrook. 1982. Molecular Cloning: A Laboratory Manual. Cold Spring Harbor Laboratory, Cold Spring Harbor, New York. 113 pp.
33. Marini, N. J., L. D. Etkin, and R. M. Benbow. 1988. Persistence and replication of plasmid DNA microinjected into early embryos of *Xenopus laevis*. *Dev. Biol.* 127:421–434.
34. Menissier, J., D. J. Hunting, and G. De Murcia. 1985. Electron microscopic mapping of single-stranded discontinuities in cauliflower mosaic virus by means of the biotin-avidin technique. *Anal. Biochem.* 148: 339–343.
35. Narayanswami, S., and B. A. Hamkalo. 1986. Electron microscopy *in situ* hybridization using biotinylated probes. *Focus* (Bethesda Research Laboratories) 8:3–6.
36. Newport, J. W., and M. W. Kirschner. 1984. Regulation of the cell cycle during early *Xenopus* development. *Cell.* 37:731–742.
37. Newport, J. 1987. Nuclear reconstitution in vitro: stages of assembly around protein-free DNA. *Cell.* 48:205–217.
38. Rochaix, J. D., A. Bird, and A. Bakken. 1974. Ribosomal RNA gene amplification by rolling circles. *J. Mol. Biol.* 87:473–487.
39. Rusconi, S., and W. Schaffner. 1981. Transformation of frog embryos with a rabbit beta-globin gene. *Proc. Natl. Acad. Sci. USA.* 78:5051–5055.
40. Watson, J. D., and F. H. C. Crick. 1953. Genetic implications of the structure of deoxyribonucleic acid. *Nature (Lond.).* 171:964–967.
41. Wickens, M. P., G. N. Buell, and R. T. Schimke. 1978. Synthesis of double-stranded DNA complementary to lysozyme, ovomucoid, and ovalbumin mRNAs. *J. Biol. Chem.* 253:2483–2495.
42. Wolf, D. P., and J. L. Hedrick. 1971. A molecular approach to fertilization. II. Viability and artificial fertilization of *Xenopus laevis*. *Dev. Biol.* 25:348–359.
43. Woodland, H. R., and R. Q. W. Pestell. 1972. Determination of the nucleoside triphosphate contents of eggs and oocytes of *Xenopus laevis*. *Biochem J.* 127:597–605.